SIAM J. APPL. MATH.
Vol. 62, No. 5, pp. 1463–1487

STABILITY OF THE STATIC SPIKE AUTOSOLITONS IN THE GRAY–SCOTT MODEL*

C. B. MURATOV† AND V. V. OSIPOV‡

Abstract. We performed an asymptotic linear stability analysis of the static spike autosolitons (ASs)—self-sustained solitary inhomogeneous states—in the Gray–Scott model of an autocatalytic chemical reaction. We found that in one dimension these ASs destabilize with respect to pulsations or the onset of traveling motion when the inhibitor is slow enough. In higher dimensions, the one-dimensional static spike ASs are always unstable with respect to corrugation and wriggling. The higher-dimensional radially symmetric static spike ASs may destabilize with respect to the radially nonsymmetric fluctuations leading to their splitting when the inhibitor is fast or with respect to pulsations when the inhibitor is slow.

Key words. pattern formation, self-organization, reaction-diffusion systems, singular perturbation theory

AMS subject classifications. 35K57, 35B52, 35B32, 35B40

PII. S0036139901384285

1. Introduction.

Self-organization and pattern formation in nonequilibrium systems are among the most fascinating phenomena in nonlinear dynamics [2, 7, 10, 20, 21, 22, 23, 25, 33]. Pattern formation is observed in various physical systems including fluids; gas and electron-hole plasmas; various semiconductor, superconductor, and gas-discharge structures; some ferroelectric, magnetic, and optical media; combustion systems (see, for example, [2, 21, 22, 23, 34]), as well as many chemical and biological systems (see, for example, [2, 7, 10, 25, 33]).

Self-organization is often associated with destabilization of the uniform state of the system [2, 22, 23]. At the same time, by applying a sufficiently strong perturbation, one can excite large-amplitude patterns, including *autosolitons* (ASs)—self-sustained solitary inhomogeneous states—when the uniform state of the system is stable [20, 21, 22, 23]. ASs are elementary objects in open dissipative systems away from equilibrium. They share properties of both solitons and traveling waves. They are similar to solitons since they are localized objects whose existence is due to nonlinearities of the system. On the other hand, from the physical point of view, they are substantially different from solitons in that they are *dissipative structures*; that is, they are self-sustained objects which form in strongly dissipative systems as a result of the balance between dissipation and pumping of energy or matter. This is the reason why, in contrast to solitons, their properties are independent of the initial conditions and are determined primarily by the nonlinearities of the system [6, 11, 15, 18, 20, 21, 22, 23]. ASs can be static, pulsating, or traveling. As a result of their various instabilities, these simplest localized patterns can spontaneously transform into complex space-filling static or dynamic patterns, including complex pulsating and traveling patterns, or spatiotemporal chaos [3, 6, 11, 12, 13, 14, 15, 16, 17, 18, 19, 20, 21, 22, 23, 27, 28, 35,

*Received by the editors January 29, 2001; accepted for publication (in revised form) November 12, 2001; published electronically May 1, 2002.
http://www.siam.org/journals/siap/62-5/38428.html
†Department of Mathematical Sciences, New Jersey Institute of Technology, University Heights, Newark, NJ 07102 (muratov@njit.edu).
‡Laboratorio de Fisica de Sistemas Pequeños y Nanotecnologia, Consejo Superior de Investigaciones Cientificas, Calle Serrano 144, 28006, Madrid, Spain (osipov@fsp.csic.es).

38]. Thus it is the destabilization of ASs that is the main source of self-organization in nonequilibrium systems with the stable homogeneous state [23].

An example of a system in which these self-organization scenarios are realized is the classical Gray–Scott reaction-diffusion model. This model describes the kinetics of a simple autocatalytic reaction in an unstirred flow reactor [8]. The reactor is a narrow space between two porous walls. Substance Y, whose concentration is kept fixed outside of the reactor, is supplied through the walls into the reactor at the rate k_0, and the products of the reaction are removed from the reactor at the same rate. Inside the reactor, Y undergoes the reaction involving an intermediate species X:

$$2X + Y \xrightarrow{k_1} 3X, \tag{1.1}$$

$$X \xrightarrow{k_2} \text{inert}. \tag{1.2}$$

The first reaction is a cubic autocatalytic reaction resulting in self-production of species X; therefore, X is the activator species. On the other hand, the production of X is controlled by species Y, so Y is the inhibitor species. The equations of chemical kinetics which describe the spatiotemporal variations of the concentrations of X and Y in the reactor and take into account the supply and removal of the substances through the porous walls take the following form:

$$\frac{\partial X}{\partial t} = -(k_0 + k_2)X + k_1 X^2 Y + D_X \Delta X, \tag{1.3}$$

$$\frac{\partial Y}{\partial t} = k_0(Y_0 - Y) - k_1 X^2 Y + D_Y \Delta Y, \tag{1.4}$$

where now X and Y are the concentrations of the activator and the inhibitor species, respectively, Y_0 is the concentration of Y in the reservoir, Δ is the two-dimensional Laplacian, and D_X and D_Y are the diffusion coefficients of X and Y.

In order to be able to understand various pattern formation phenomena in a system of this kind, it is crucial to introduce the variables and the time and length scales that best represent the physical processes acting in the system. First and most important is the choice of the characteristic time scales. These are primarily dictated by the time constants of the dissipation processes. For Y, this is the supply and the removal with the rate k_0, whereas for X this is the removal from the system and the decay via the second reaction with the total rate $k_0 + k_2$. The natural way to introduce the dimensionless inhibitor concentration is to scale it with Y_0. Since we want to fix the time scale of the variation of the inhibitor (with the fixed activator), we will rescale X in such a way that the reaction term in (1.4) will generate the same time scale as the dissipative term. This leads to the following dimensionless quantities:

$$\theta = X/X_0, \quad \eta = Y/Y_0, \quad X_0 = \left(\frac{k_0}{k_1}\right)^{1/2}. \tag{1.5}$$

The characteristic time and length scales for these quantities are

$$\tau_\theta = (k_0 + k_2)^{-1}, \; \tau_\eta = k_0^{-1}, \tag{1.6}$$

$$l = (D_X \tau_\theta)^{1/2}, \quad L = (D_Y \tau_\eta)^{1/2}. \tag{1.7}$$

Naturally, one should require positivity of θ and η.

Let us measure length and time in the units of l and τ_θ, respectively. Then (1.3) and (1.4) can be rewritten in the dimensionless form as follows:

$$\frac{\partial\theta}{\partial t} = \Delta\theta + A\theta^2\eta - \theta, \tag{1.8}$$

$$\alpha^{-1}\frac{\partial\eta}{\partial t} = \epsilon^{-2}\Delta\eta - \theta^2\eta + 1 - \eta, \tag{1.9}$$

where we introduced the following dimensionless parameters:

$$\epsilon = \left(\frac{k_0 D_X}{(k_0+k_2)D_Y}\right)^{1/2}, \quad \alpha = \frac{k_0}{k_0+k_2}, \quad A = \frac{Y_0 k_0^{1/2} k_1^{1/2}}{(k_0+k_2)}. \tag{1.10}$$

The parameters $\epsilon = l/L$ and $\alpha = \tau_\theta/\tau_\eta$ are the ratios of the length and time scales of the activator and the inhibitor, respectively, and A characterizes the degree of deviation of the system from thermal equilibrium.

For $A < 2$, the system has only one homogeneous state $\theta = \theta_h$, $\eta = \eta_h$, where

$$\theta_h = 0, \quad \eta_h = 1, \tag{1.11}$$

whereas for $A \geq 2$ two other homogeneous states appear:

$$\theta_{h2,3} = \frac{A \mp \sqrt{A^2-4}}{2}, \quad \eta_{h2,3} = \frac{A \pm \sqrt{A^2-4}}{2A}. \tag{1.12}$$

It is easy to see that the homogeneous state $\theta = \theta_h$, $\eta = \eta_h$ is stable for all values of the system's parameters. Thus self-organization associated with the Turing instability of the homogeneous state $\theta_h = 0$ and $\eta_h = 1$ is not realized in the Gray–Scott model. Instead, for $A < 2$, self-organization may occur only as a result of the instabilities of large-amplitude patterns already present in the system.

Let us emphasize that ϵ or α are the natural small parameters in systems of this kind. Their relative smallness is in fact a necessary condition for the feasibility of any patterns in systems with a unique homogeneous state [6, 11, 12, 13, 14, 15, 18, 20, 21, 22, 23]. Indeed, if the inverse were true, that is, if both the characteristic time and length scales of the variation of the inhibitor were much smaller than those of the activator, the inhibitor would easily damp all the deviations of the activator from the homogeneous state, making the formation of any kinds of persistent patterns impossible. This can be easily seen in the Gray–Scott model with $\epsilon \gg 1$ and $\alpha \gg 1$. In this case, (1.9) reduces (on the time scales of order 1) to $\eta = 1/(1+\theta^2)$. Substituting this into (1.8), we obtain

$$\frac{\partial\theta}{\partial t} = \Delta\theta + \frac{A\theta^2}{1+\theta^2} - \theta. \tag{1.13}$$

This equation possesses a simple variational structure

$$\frac{\partial\theta}{\partial t} = -\frac{\delta\mathcal{F}}{\delta\theta}, \quad \mathcal{F} = \int d^d x \left(\frac{(\nabla\theta)^2}{2} - A\theta + A\arctan\theta + \frac{\theta^2}{2}\right). \tag{1.14}$$

For $A < 2$, the functional $\mathcal{F}$ has a unique global minimum at $\theta = \theta_h = 0$, so any initial condition will evolve to the homogeneous state θ_h. For $A > 2$, there are two stable homogeneous states $\theta = \theta_h$ and $\theta = \theta_{h3}$ (see above), so it is possible to have waves of switching from one homogeneous state to the other [2]. It is easily checked

that, in such a wave, the homogeneous state θ_h invades θ_{h3} when $2 < A < 2.18$, while for $A > 2.18$ the homogeneous state θ_{h3} invades θ_h.

Thus pattern formation in the Gray–Scott model is possible only when $\epsilon \lesssim 1$ and/or $\alpha \lesssim 1$. Therefore, it is advantageous to consider the extreme cases $\epsilon \ll 1$ and/or $\alpha \ll 1$. In [30], we showed that when $\epsilon \ll 1$, one can excite static spike ASs in the Gray–Scott model in one, two, and three dimensions. These ASs have the form of spikes of width of order 1 (in our units) and large amplitude in the distribution of θ. For sufficiently small ϵ, Doelman, Kaper, and Zegeling proved existence of these solutions in a certain parameter range in one dimension [5], and Wei proved the existence of radially symmetric solutions in a certain parameter range in two dimensions [41]. Hale, Peletier, and Troy constructed stationary solutions and studied their stability in the Gray–Scott model with $\epsilon \simeq 1$ [9].

In the present paper, we perform a comprehensive asymptotic analysis of the linear stability of the static spike ASs in the Gray–Scott model in one, two, and three dimensions for $\epsilon \ll 1$. Our paper is organized as follows. In section 2, we study stability of the one-dimensional static spike AS in higher dimensions, in section 3 we do that for the three-dimensional radially symmetric static spike AS, in section 4 we outline the stability analysis of the two-dimensional radially symmetric static spike AS, and in section 5 we summarize our results.

2. Stability of the one-dimensional static spike AS. We start by analyzing the one-dimensional static spike AS in higher dimensions. In one dimension, the solution in the form of the static AS exists for $A_b \le A \le A_d$, where $A_b = \sqrt{12\epsilon}$ and $A_d \simeq 1.35$ for $\epsilon \ll 1$. For $A_b \le A \ll A_d$, the inner solutions $\tilde\theta$, $\tilde\eta$ describing the spike region are [30]

$$\tilde\theta = \frac{3\epsilon A}{A_b^2}\left[1+\sqrt{1-\frac{A_b^2}{A^2}}\right]\cosh^{-2}\left(\frac{x}{2}\right), \quad \tilde\eta = \frac{A_b^2}{2\epsilon A^2}\left[1+\sqrt{1-\frac{A_b^2}{A^2}}\right]^{-1}. \tag{2.1}$$

For $A_b \ll A \ll A_d$, these functions become $\tilde\theta = \frac{A}{2}\cosh^{-2}\left(\frac{x}{2}\right)$ and $\tilde\eta = \frac{3}{A^2}$. For $A \sim A_d$, the inner solutions are found numerically.

The equations describing small deviations $\delta\theta = \theta - \theta_0$ and $\delta\eta = \eta - \eta_0$ of the activator and the inhibitor, respectively, from the distributions $\theta_0(x)$ and $\eta_0(x)$ in the form of the static one-dimensional AS are obtained by linearizing (1.8) and (1.9). (We chose the axes so that θ_0 and η_0 depend only on x.) Let us take

$$\delta\theta = \delta\theta_{k\omega}(x)e^{\mathrm{i}\omega t - \mathrm{i}ky}, \quad \delta\eta = \delta\eta_{k\omega}(x)e^{\mathrm{i}\omega t - \mathrm{i}ky}, \tag{2.2}$$

where ω is the complex frequency and k is the wave vector that characterizes the transverse perturbations of the AS. Then, after some algebra, (1.8) and (1.9) linearized around θ_0 and η_0 can be written as

$$\left[-\frac{d^2}{dx^2} + 1 + \mathrm{i}\omega + k^2 - 2A\theta_0\eta_0\right]\delta\theta_{k\omega} = A\theta_0^2\delta\eta_{k\omega}, \tag{2.3}$$

$$\left[-\epsilon^{-2}\frac{d^2}{dx^2} + 1 + \mathrm{i}\alpha^{-1}\omega + \epsilon^{-2}k^2\right]\delta\eta_{k\omega} = -A^{-1}\left[-\frac{d^2}{dx^2} + 1 + \mathrm{i}\omega + k^2\right]\delta\theta_{k\omega}. \tag{2.4}$$

Equation (2.4) can be solved by means of Green's function

$$\delta\eta_{k\omega} = -\frac{\epsilon^2}{A}\delta\theta_{k\omega} - \frac{\epsilon\left(1-\epsilon^2+\mathrm{i}\omega-\mathrm{i}\epsilon^2\alpha^{-1}\omega\right)}{2A\sqrt{1+\mathrm{i}\alpha^{-1}\omega+\epsilon^{-2}k^2}}\int_{-\infty}^{+\infty} e^{-\epsilon\sqrt{1+\mathrm{i}\alpha^{-1}\omega+\epsilon^{-2}k^2}|x-x'|}\delta\theta_{k\omega}(x')dx'. \tag{2.5}$$

This expression for $\delta\eta_{k\omega}$ can be substituted back into (2.3) to get a single integro-differential equation in terms of $\delta\theta_{k\omega}$ alone:

$$\left[-\frac{d^2}{dx^2}+1+\mathrm{i}\omega+k^2-2A\theta_0\eta_0+\epsilon^2\theta_0^2\right]\delta\theta_{k\omega} = -\frac{\epsilon(1-\epsilon^2+\mathrm{i}\omega-\mathrm{i}\epsilon^2\alpha^{-1}\omega)\theta_0^2}{2\sqrt{1+\mathrm{i}\alpha^{-1}\omega+\epsilon^{-2}k^2}}\int_{-\infty}^{+\infty} e^{-\epsilon\sqrt{1+\mathrm{i}\alpha^{-1}\omega+\epsilon^{-2}k^2}|x-x'|}\delta\theta_{k\omega}(x')dx'. \tag{2.6}$$

Equation (2.6) is the basic equation for studying the stability of the static one-dimensional AS in higher dimensions. One has to solve this equation as an eigenvalue problem: find the modes $\delta\theta_n$ and the values of $\omega = \omega_n(k)$ corresponding to them. The instability of the AS will occur when the real part of $\gamma = -\mathrm{i}\omega$ is negative. (Re γ is the damping decrement (decay rate) of a fluctuation.) We will use ω and γ interchangeably throughout this paper. To analyze the stability of the static spike AS in one dimension, one should simply put $k = 0$ in (2.6).

Note that since θ_0^2 in the right-hand side of (2.6) is an exponentially decaying function of x [30], a mode $\delta\theta_n$ can be unstable only if it is localized, since otherwise we would have $\gamma = 1 + k^2 > 0$. In other words, the unstable modes should be in the *discrete* spectrum of the solutions of (2.6). Also note that since the static AS is symmetric with respect to its center, the spectrum of the problem breaks up into even and odd modes. For the purposes of notation, we will choose even (odd) values of a nonnegative integer n to denote the even (odd) modes $\delta\theta_n$ ordered by Re γ_n. Because of the translational invariance, the problem always has a zero eigenvalue with the corresponding odd eigenfunction $\delta\theta = d\theta_0/dx$. The analysis below shows that qualitatively the first few modes $\delta\theta_n$ look like those shown in Figure 2.1.

Observe that the operator in the left-hand side of (2.6) is a Schrödinger-type operator with the potential in the form of a well of depth and size of order 1. Indeed, according to the results of [30], the characteristic length scale of the variation of θ_0 is of order 1, and we have $\theta_0 \sim A\epsilon^{-1}$ and $\eta_0 \sim A^{-2}\epsilon$ in the spike, and so $A\theta_0\eta_0 \sim 1$ and exponentially decays away from the spike. Also, the right-hand side of (2.6) is multiplied by the function θ_0^2, which also exponentially decays away from the spike. Therefore, in solving this eigenvalue problem, one should know only the distributions θ_0 and η_0 in the spike. So, for $\epsilon \ll 1$, we may use only the inner solutions $\tilde\theta$ and $\tilde\eta$ obtained in [30] and set $\theta_0 = \epsilon^{-1}\tilde\theta$ and $\eta_0 = \epsilon\tilde\eta$ in (2.6).

2.1. Case $\alpha \gg 1$ and $k = 0$: Stability of the AS in one dimension. According to the general qualitative theory of ASs, the static spike AS should be stable in the entire region of its existence for $\alpha \gg 1$ in one dimension [21, 22, 23]. To see this, let us analyze (2.6) in the case $\alpha \gg 1$ and $k = 0$. In this case, it can be asymptotically written as

$$\left[-\frac{d^2}{dx^2}+1-\gamma-2A\tilde\theta\tilde\eta+\tilde\theta^2\right]\delta\theta = -\frac{1}{2\epsilon}\tilde\theta^2(1-\gamma)\int_{-\infty}^{+\infty}\delta\theta(x')dx'. \tag{2.7}$$

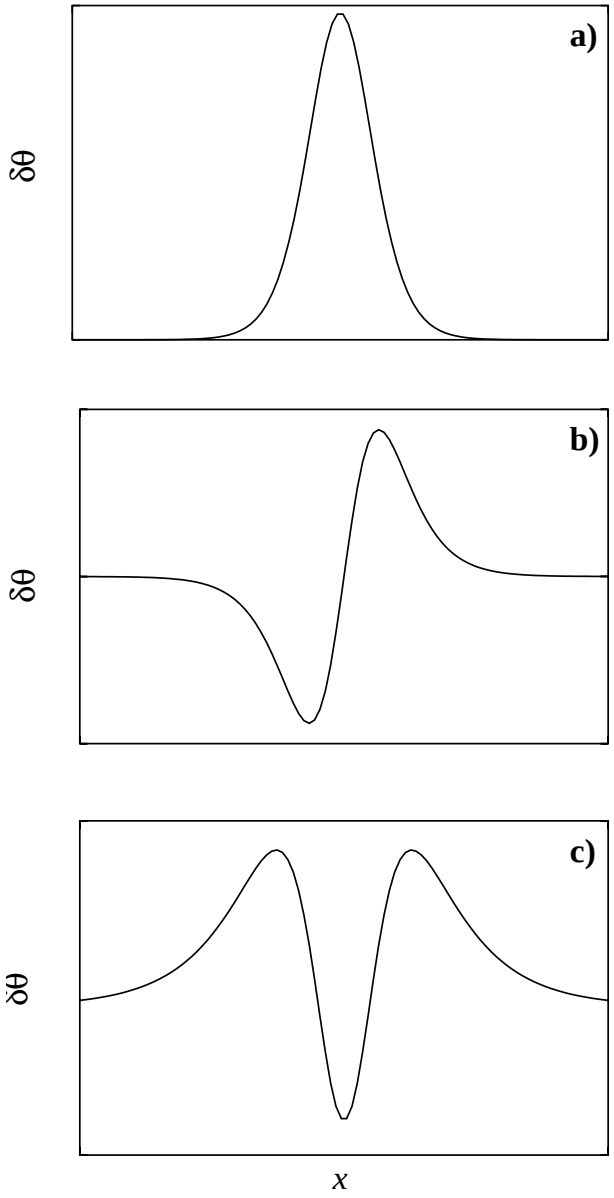

FIG. 2.1. *A qualitative form of the lowest-lying modes* $\delta\theta_n$.

To see that the AS is stable in one dimension for $A_b \ll A < A_d$ in the case of sufficiently large α, we solved (2.7) numerically, using the asymptotic distributions $\tilde{\theta}$ and $\tilde{\eta}$ obtained in [30]. We solve this equation by discretizing the operators and diagonalizing the obtained matrices for sufficiently small ϵ. This gives γ_n as functions of A.

We found that the discrete spectrum of the problem contains at least one even eigenvalue. The damping decrement Re γ_0 is positive and goes to zero as $A \to A_d$, signifying the instability of the AS at this point. The corresponding eigenfunction has two nodes with two distinct peaks and a deep trough between them (Figure 2.2(a)),

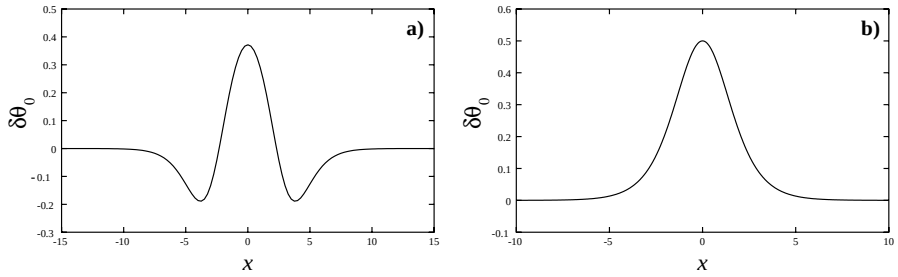

FIG. 2.2. *The form of the critical fluctuation* $\delta\theta_0$ *at* $A = A_d$ (a) *and* $A = A_b$ (b).

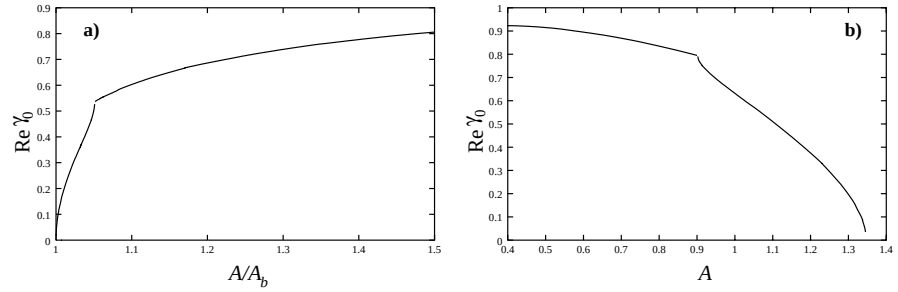

FIG. 2.3. *The dependence* $\mathrm{Re}\,\gamma_0(A)$ *for the static one-dimensional AS for* $A \sim A_b$ (a) *obtained from the numerical solution of* (2.8)*, and* $A \sim A_d$ (b) *obtained from* (2.7).

suggesting that the instability at $A = A_d$ will result in the local breakdown in the AS center and its splitting. The latter is supported by the numerical simulations [29, 39, 40].

When $A \sim A_b$, (2.7) can be further simplified by using the analytical expressions for $\tilde{\theta}$ and $\tilde{\eta}$ from (2.1) [30] and ignoring the last term in the square bracket in its left-hand side. So, (2.7) in the case $A \sim A_b$ asymptotically becomes

$$\left[-\frac{d^2}{dx^2} + 1 - \gamma - 3\cosh^{-2}\left(\frac{x}{2}\right)\right]\delta\theta = -\frac{3A^2(1-\gamma)}{8A_b^2}\left[1 + \sqrt{1 - \frac{A_b^2}{A^2}}\right]^2 \cosh^{-4}\left(\frac{x}{2}\right)\int_{-\infty}^{+\infty}\delta\theta(x')dx'. \tag{2.8}$$

Naturally, (2.7) in the case $A \ll 1$ should give the same results as (2.8) in the case $A \gg A_b$. The numerical analysis of this equation also shows that the damping decrement $\mathrm{Re}\,\gamma_0 > 0$ for $A > A_b$ and that $\gamma_0 \to 0$ as A approaches A_b. By direct inspection, the corresponding eigenfunction at $A = A_b$ is $\delta\theta_0 = \cosh^{-2}(x/2)$. It has only one peak (Figure 2.2(b)) and no nodes and results in the AS collapse at this value of A [29].

The damping decrements $\mathrm{Re}\,\gamma_0(A)$ obtained from the numerical solution of (2.7) and (2.8) are shown in Figure 2.3. This figure indicates that for sufficiently large α the static spike AS in one dimension is indeed stable in the entire region of its existence. Notice that it turns out that only at $A_b < A < 1.06A_b$ or at $0.90 < A < A_d$ we have $\mathrm{Re}\,\omega_{0,2} = 0$ so that there are two distinct localized modes $\delta\theta_{0,2}$ with different (real)

values of γ. For all other values of A, we have Re $\omega \neq 0$, and there are two complex-conjugate eigenfunctions corresponding to the two complex frequencies ω and $-\omega^*$. For $A_b \ll A \ll A_d$, we have Re $\gamma_0 \simeq 1$ and Re $\omega_0 \simeq 0.15$.

Observe that (2.8) can be analyzed rigorously. This analysis turns out to be rather involved, so we present it in Appendix A. It agrees with the conclusions of this section concerning the case $A \ll 1$. Note that Doelman, Gardner, and Kaper independently showed stability of the one-dimensional static spike AS in a limited region of the parameters by a direct solution of an equation equivalent to (2.8) [4].

2.2. Case $\alpha \lesssim 1$ and $k = 0$: Instability with respect to pulsations. The general qualitative theory of ASs suggests that for small enough values of α the static spike AS may become unstable with respect to the fluctuations with Re $\omega \neq 0$, resulting in the onset of the AS pulsations [21, 22, 23]. The analysis of (2.6) shows that, in order for it to have a solution with Im $\omega = 0$ and Re $\omega = \omega_0 \neq 0$, we must have $\epsilon^2 \lesssim \alpha \lesssim 1$ and $\omega_0 \sim 1$. Let us introduce $\kappa^2 = \epsilon^2/\alpha \lesssim 1$. Then, dropping 1 in the square roots in the right-hand side of (2.6) and putting $k = 0$, we get asymptotically

$$\left[-\frac{d^2}{dx^2} + 1 + \mathrm{i}\omega_0 - 2A\tilde{\theta}\tilde{\eta} + \tilde{\theta}^2\right]\delta\theta = -\frac{(1 + \mathrm{i}\omega_0 - \mathrm{i}\kappa^2\omega_0)\tilde{\theta}^2}{2\kappa\sqrt{\mathrm{i}\omega_0}} \int_{-\infty}^{+\infty} e^{-\kappa\sqrt{\mathrm{i}\omega_0}|x-x'|}\delta\theta(x')dx'. \tag{2.9}$$

In order for the exponential in the right-hand side of this equation to decay at large distances, we must choose the analytic branch of the square root that has a positive real part for all values of ω_0, which is achieved by making a branch cut along the positive imaginary axis. Strictly speaking, the branch cut should begin at $\omega = i\alpha$ (see (2.6) with $k = 0$), which for sufficiently small α can be considered to be at zero in the analysis of the dangerous modes.

To find the instabilities of the static spike AS with respect to pulsations, we first solved (2.9) numerically using the inner solutions of [30] for $A \sim 1$. This numerical solution shows that the static spike AS indeed becomes unstable with respect to the fluctuation $\delta\theta_0$, which looks like Figure 2.1(a), with Re $\omega = \omega_0(A)$ at $\alpha < \alpha_\omega(A) \sim \epsilon^2$. The plots of $\alpha_\omega(A)$ and $\omega_0(A)$ are shown in Figures 2.4(a) and 2.4(b), respectively. Alternatively, for a given value of $\alpha \sim \epsilon^2$, the static spike AS becomes unstable with respect to pulsations when $A < A_\omega \lesssim 1$.

Equation (2.9) can be simplified in the case $A_b \ll A \ll 1$ and $\epsilon^2 \ll \alpha \ll 1$. In this case, one can use the analytical expressions from (2.1) for $\tilde{\theta}$ and $\tilde{\eta}$ in the limit $A \gg A_b$ and neglect the last term in the left-hand side of (2.9), the exponential, and the term $\mathrm{i}\kappa^2\omega_0$ in its right-hand side. As a result, (2.9) can be written in this case as

$$\left[-\frac{d^2}{dx^2} + 1 + \mathrm{i}\omega_0 - 3\cosh^{-2}\left(\frac{x}{2}\right)\right]\delta\theta = -\frac{A^2(1 + \mathrm{i}\omega_0)\cosh^{-4}(x/2)}{8\kappa\sqrt{\mathrm{i}\omega_0}} \int_{-\infty}^{+\infty} \delta\theta(x')dx'. \tag{2.10}$$

One can see that the dependence on the system's parameters enters this equation via only the combination $A^2/\kappa = \alpha^{1/2}A^2/\epsilon$. Solving (2.10) numerically, we obtain that the AS destabilizes at

$$\alpha_\omega = 5.15 \times \epsilon^2 A^{-4}, \quad \omega_0 = 0.534, \quad \text{for } A_b \ll A \ll 1. \tag{2.11}$$

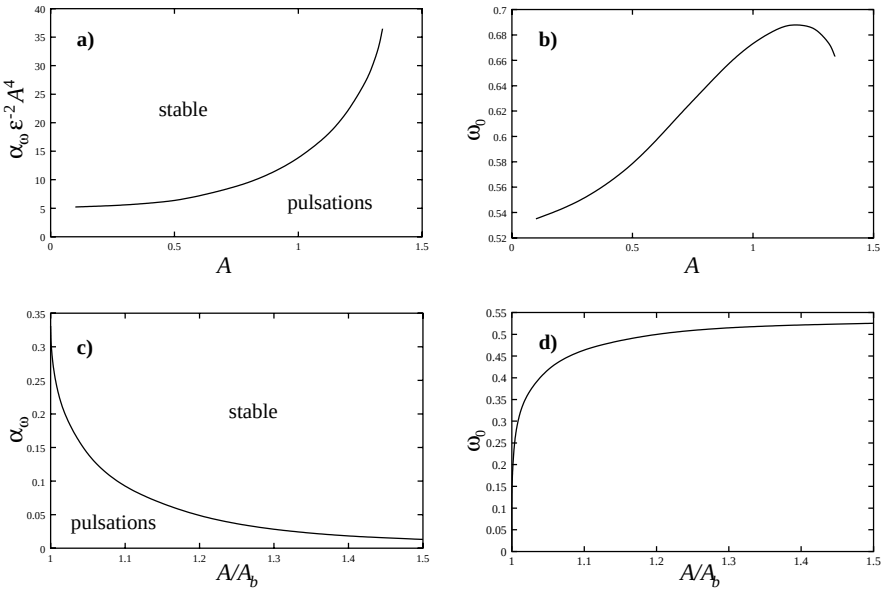

FIG. 2.4. *The dependences* $\alpha_\omega(A)$ (a) *and* $\omega_0(A)$ (b) *for the static one-dimensional AS obtained from the numerical solution of* (2.9)*; the dependences* $\alpha_\omega(A)$ (c) *and* ω_0 (d) *are obtained from the numerical solution of* (2.13).

Note that (2.10) can be rigorously analyzed by the method similar to the one used for (2.8). This analysis is presented in Appendix B. It yields the same conclusions as above and in (2.11). The result of (2.11) is in agreement with that of Doelman, Gardner, and Kaper obtained by a direct solution of an equation equivalent to (2.10) in a limited parameter region [4]. Notice that this equation gives a good approximation for α_ω only for $A \lesssim 0.5$ (see Figure 2.4(a)). Recalling that we must have $A \gg A_b = \sqrt{12\epsilon}$, we see that (2.11) can give a good approximation only for $\epsilon \lesssim 0.01$ in a limited range of A.

For $A_b \ll A \ll 1$ and $\epsilon^2 \ll \alpha \ll \alpha_\omega$, it is easy to show that the AS is unstable. For these values of A and α, the right-hand side of (2.10) is a perturbation, so to the leading order $\delta\theta_0$ is given by (A.2). The solution of (2.10) in the first order of perturbation theory with $\alpha/\epsilon^2 \ll A^4$ then gives us

$$\gamma_0 \simeq -\frac{5}{4} + \frac{27\pi^2\sqrt{5}}{1024} A^2 \alpha^{1/2} \epsilon^{-1} < 0. \tag{2.12}$$

Notice that by equating this expression to zero, one gets the value of α which differs from α_ω given by (2.11) by only 10%.

According to (2.11), when A decreases, the value of α_ω increases, and when A reaches the value of order A_b, we must have $\alpha_\omega \sim 1$, and so for these values of the parameters one can no longer neglect 1 compared to $\alpha^{-1}\omega$ in the square roots in (2.6). On the other hand, in this case, one can still use the same approximations as in deriving (2.10), except we should now use the asymptotic expressions for $\tilde{\theta}$ and $\tilde{\eta}$

from (2.1) [30]. As a result, for $\alpha \sim 1$ and $A \sim A_b$, we get asymptotically

$$\left[-\frac{d^2}{dx^2} + 1 + \mathrm{i}\omega_0 - 3\cosh^{-2}\left(\frac{x}{2}\right)\right]\delta\theta = -\frac{3A^2(1+\mathrm{i}\omega_0)}{8A_b^2\sqrt{1+\mathrm{i}\alpha^{-1}\omega_0}}\left[1+\sqrt{1-\frac{A_b^2}{A^2}}\right]^2 \cosh^{-4}\left(\frac{x}{2}\right)\int_{-\infty}^{+\infty}\delta\theta(x')dx'. \tag{2.13}$$

The results of the numerical solution of this equation for α_ω and ω_0 are presented in Figures 2.4(c) and 2.4(d), respectively. From these figures, one can see that for $\alpha > \alpha_0 \simeq 0.33$ the considered instability of the static spike AS cannot be realized for any value of A. This result is in agreement with the general qualitative theory of ASs [21, 22, 23].

2.3. Case $\alpha \gg 1$ and $k \neq 0$: Instability with respect to corrugation. Let us now see what happens in higher dimensions when $A \sim 1$ and α is sufficiently large (so that the terms proportional to α^{-1} in (2.6) can be dropped) as the value of k is varied. Let us consider the situation when $\epsilon \ll k \lesssim 1$. Then one can neglect 1 compared to $\epsilon^{-2}k^2$ in the square roots in (2.6) and write it asymptotically as

$$\left[-\frac{d^2}{dx^2} + 1 - \gamma_k + k^2 - 2A\tilde{\theta}\tilde{\eta} + \tilde{\theta}^2\right]\delta\theta_k = -\frac{\tilde{\theta}^2(1-\gamma_k)}{2k}\int_{-\infty}^{+\infty} e^{-k|x-x'|}\delta\theta_k(x')dx'. \tag{2.14}$$

Note that for $k \sim 1$ the coefficient multiplying the right-hand side of (2.14) becomes of order 1. Here we should expect a corrugation instability with respect to the mode $\delta\theta_0$ with some $k = k_0 \sim 1$ [21, 22, 23, 36]. Indeed, as the value of k increases, the magnitude of the right-hand side of (2.6) decreases as $1/k$, while the contribution to the left-hand side of (2.6) increases as k^2. Therefore, for some $k = k_0$, the contribution of both these two terms to (2.6) will be minimal so that we can get an instability: $\mathrm{Re}\,\gamma_{k_0} < 0$.

To show that there is indeed an instability at $k \sim 1$, we solved (2.14) numerically using the asymptotic distributions for $\tilde{\theta}$ and $\tilde{\eta}$ obtained in [30]. Figure 2.5 shows the solutions for $\mathrm{Re}\,\gamma_k$ obtained for a particular value of $A = 1.2$.

For $k > 0.29$, (2.14) has two localized even solutions and a continuous spectrum of γ_k for $A = 1.2$, all having $\mathrm{Re}\,\omega(k) = 0$. The curve at the bottom of the figure corresponds to $\delta\theta_0$, the curve in the middle corresponds to $\delta\theta_2$, and the curve on the top is the bottom of the continuous spectrum. The corresponding eigenmodes look like Figures 2.1(a) and 2.1(c), respectively. From Figure 2.5, one can see that the AS is unstable with respect to $\delta\theta_0$ (the corrugation instability) for a range of wave vectors $k \sim 1$. When $0.05 < k < 0.29$, the complex frequency $\omega(k)$ for the modes $\delta\theta_{0,2}$ acquires a real part for $A = 1.2$. The corresponding eigenfunctions for these modes, as well as γ_k, are complex-conjugate. The real and the imaginary parts of these eigenmodes look like linear combinations of the functions shown in Figures 2.1(a) and 2.1(c). For yet smaller values of k, the real part of ω vanishes once again, so we have two distinct solutions, with $\delta\theta_0$ and $\delta\theta_2$ looking like Figures 2.1(c) and 2.1(a), respectively. The latter is related to the presence of two distinct solutions in the case of the one-dimensional AS studied in section 2.1, which is obtained from

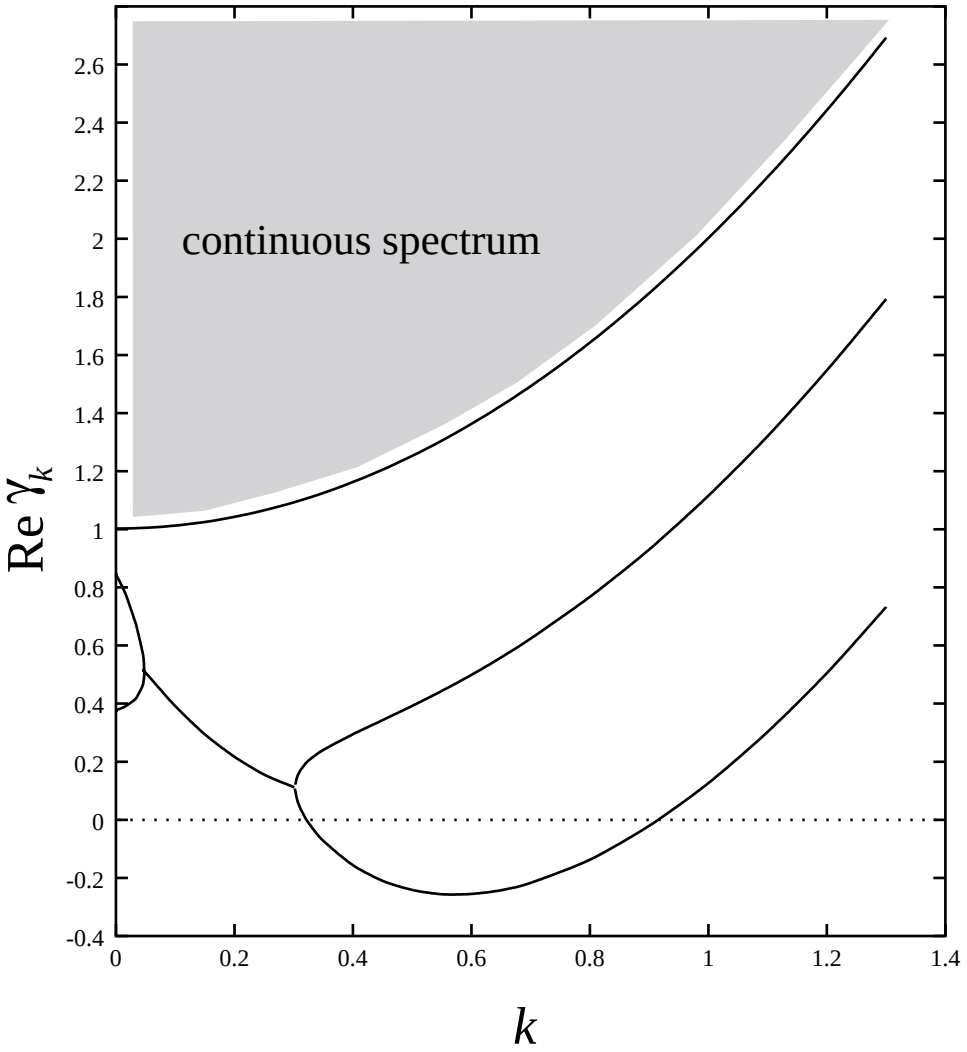

FIG. 2.5. *The damping decrement* Re γ_k *for the static one-dimensional AS obtained from the numerical solution of* (2.14) *for different modes at* $A = 1.2$.

(2.14) in the limit $k \to 0$. When the value of A is decreased below $A = 0.90$, these two distinct solutions disappear, and the solution with a nonzero real part of $\omega(k)$ goes all the way to $k = 0$.

The analysis of γ_k for different values of A shows that the static one-dimensional spike AS in higher dimensions is unstable with respect to corrugation for all values of A at which it exists. Note that, in the case $A_b \ll A \ll 1$, it can be easily shown that the AS is unstable with respect to the corrugation instability. Indeed, for $A \ll 1$ and $A^2 \ll k \ll 1$, the inner solution is given by (2.1) in the limit $A \gg A_b$, so one can neglect the exponential in the right-hand side and the last term in the bracket in the left-hand side of (2.14). Then the operator in the right-hand side of (2.14) is a perturbation, so, in the zeroth approximation, $\delta\theta_0$ is given by (A.2). Then, in the

first order of perturbation theory,

$$\gamma_0(k) = \left(-\frac{5}{4} + \frac{75\pi^2 A^2}{2048k} + k^2\right)\left(1 + \frac{75\pi^2 A^2}{2048k}\right)^{-1}, \tag{2.15}$$

which is negative for $A^2 \ll k \lesssim 1$. The same conclusion can be made for $A \sim A_b$ along the same arguments. Notice that according to (2.15) the fastest growing mode has $k \simeq 0.60$, which coincides with very good accuracy with the results of the numerical solution of (2.14) (see Figure 2.5).

2.4. Case $\alpha \gg 1$ and $k \neq 0$: Instability with respect to wriggling. Let us now turn to the mode $\delta\theta_1$. The numerical analysis of (2.7), which determines the stability of the static AS in one dimension for $\alpha \gg 1$, shows that, for $k = 0$, we have $\gamma_1 = 0$ and $\delta\theta_1 = d\tilde{\theta}/dx$ corresponding to the translational mode. This mode looks like the one shown in Figure 2.1(b). Since this mode is degenerate, it is of special interest to study the solutions of (2.6) for $|\gamma| \ll 1$ and $k \ll 1$. The small values of k and γ introduce a weak perturbation to the operators in (2.6) with $k = 0$ and $\gamma = 0$. Therefore, in the leading order of perturbation theory, we must multiply (2.6) by the adjoint function $\delta\theta_1^*$ and integrate over x. As a result, in the first order in γ_k and k^2, we obtain

$$\begin{aligned} &-\gamma_k + k^2 + \frac{\gamma_k}{2}(1 - \epsilon^2\alpha^{-1}) \int_{-\infty}^{+\infty} \int_{-\infty}^{+\infty} \tilde{\theta}^2(x)\delta\theta_1^*(x)|x - x'|\delta\theta_1(x')dxdx' \\ &\qquad = \frac{\epsilon}{8\alpha}(\gamma_k - \alpha\epsilon^{-2}k^2) \int_{-\infty}^{+\infty} \int_{-\infty}^{+\infty} \tilde{\theta}^2(x)\delta\theta_1^*(x)(x - x')^2\delta\theta_1(x')dxdx', \end{aligned} \tag{2.16}$$

where we expanded the exponential in (2.6) up to the second order in ϵ and used the normalization $\int_{-\infty}^{+\infty} \delta\theta_1^*\delta\theta_1 dx = 1$.

Recalling that $\delta\theta_1 = d\tilde{\theta}/dx$, we can calculate the integral in the right-hand side of (2.16). Using the symmetry properties of $\delta\theta_1$, we find this integral to be $2\int_{-\infty}^{+\infty} x\tilde{\theta}^2\delta\theta_1^* dx \int_{-\infty}^{+\infty} \tilde{\theta} dx$. For $A_b \ll A \leq A_d$, we used the inner solutions obtained in [30] to compute $\delta\theta_1^*$ numerically and found that this integral is negative for all values of A. By a similar integration, one can show that the integral in the left-hand side of (2.16) is also negative. Then, it is easy to see that when $\alpha \gtrsim \epsilon$ (otherwise, the AS would be unstable in one dimension (see section 2.5 below)), for small values of k, we will have $\gamma_1(k) \sim -\epsilon^{-1}A^2k^2 < 0$, so the one-dimensional static spike AS is in fact always unstable with respect to the $\delta\theta_1$ mode with small k for $A \gg A_b$. These fluctuations lead to wriggling of the AS [29, 32].

Moreover, it is possible to show that the static spike AS which is stable in one dimension is in fact unstable with respect to wriggling for all values of $A > A_b$. Indeed, for $A \sim A_b$, the operator in the right-hand side of (2.6), which is the only non-self-adjoint operator there, can be considered as a perturbation, and so to the leading order $\delta\theta_1^* = \delta\theta_1$, where $\delta\theta_1$ is given by (A.2) and $\tilde{\theta}$ is given by (2.1). Substituting this into (2.16), we obtain that for small values of k the damping decrement γ_k of the fluctuations leading to wriggling is given by

$$\gamma_1(k) \simeq k^2\left[1 - \frac{A^2}{A_b^2}\left(1 + \sqrt{1 - \frac{A_b^2}{A^2}}\right)^2\right]. \tag{2.17}$$

From this equation, one can see that $\gamma_1(k) < 0$ for small k, signifying an instability, for $A > A_b$, and sufficiently small k. Thus, in summary, the one-dimensional static

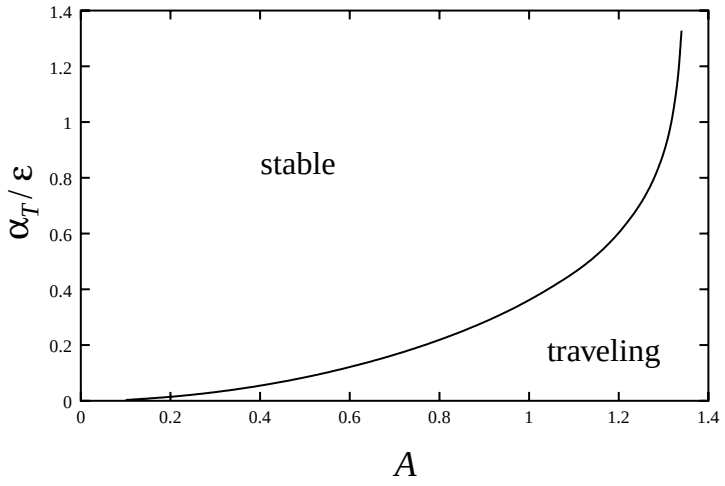

FIG. 2.6. *The dependence $\alpha_T(A)$ for the static one-dimensional AS obtained from the numerical solution of* (2.16).

spike AS is always unstable in higher dimensions, and so the instabilities that are realized for sufficiently small α are meaningful only for the one-dimensional system. Note that the wriggling instability was found in [37] for a simplified version of the Gray–Scott model.

2.5. Case $\alpha \ll 1$ and $k = 0$: Instability with respect to the onset of traveling motion. In addition to the instability of the AS with respect to wriggling, another instability may be realized when $\alpha \ll 1$ [37]. As was already mentioned, for $k = 0$, (2.16) has a simple zero solution for any α due to the translational invariance. However, at some special value of $\alpha = \alpha_T$, the solution $\gamma = 0$ may become doubly degenerate. This will happen when the coefficient in front of γ in (2.16) vanishes. If this is the case, in addition to the trivial solution, we will have another nontrivial zero solution, for which the value of γ should *change sign* as the value of α passes through α_T. This signifies an instability that leads to the onset of traveling motion. It is not difficult to see that this instability will occur when $\alpha < \alpha_T \sim \epsilon$ for $A \lesssim 1$. In particular, when $A \ll 1$, we can put $\delta\theta_1^* = \delta\theta_1$, where $\delta\theta_1$ is given by (A.2), since again the only non-self-adjoint operator is the operator in the right-hand side of (2.6) and is small. After a little algebra, we obtain that the instability will occur at

$$\alpha_T = \begin{cases} \frac{\epsilon^2 A^2}{A_b^2}\left[1+\sqrt{1-\frac{A_b^2}{A^2}}\right]^2, & A \sim A_b, \\ \frac{1}{3}A^2\epsilon, & A_b \ll A \ll 1. \end{cases} \tag{2.18}$$

Note that the last formula coincides with the expression for the bifurcation point between the traveling and the static spike AS obtained by us in [29, 31].

To analyze the dependence $\alpha_T(A)$ for $A \sim 1$, we solved for the adjoint function $\delta\theta_1^*$ numerically and then substituted it into (2.16). The resulting dependence $\alpha_T(A)$ is presented in Figure 2.6. Observe that for $A < 1$ the value of α_T is given by (2.18) with an accuracy better than 10%.

2.6. Comparison of the pulsation and traveling instabilities. According to (2.11) and (2.18), for $A > 1.58\epsilon^{1/6}$, we have $\alpha_T > \alpha_\omega$, so if one starts with the static spike AS at $A \sim 1$ and a sufficiently large value of α and then gradually decreases α, the AS will destabilize with respect to the fluctuation $\delta\theta_1$ that looks like Figure 2.1(b) and transform into traveling. If, on the other hand, we have $A < 1.58\epsilon^{1/6}$ at the start, the AS will destabilize with respect to pulsations, with the corresponding eigenmode looking like Figure 2.1(a). Also, according to (2.11) and (2.18), for $\alpha < \alpha_c = 0.83\epsilon^{4/3}$, the one-dimensional static spike AS will be unstable regardless of the value of A, and so we conclude that this AS can be excited only when $\alpha > \alpha_c$.

3. Stability of the three-dimensional radially symmetric static spike AS. Let us now turn to the three-dimensional radially symmetric spike ASs. It turns out that, up to the logarithmic terms, all the results on the stability of the two- and three-dimensional radially symmetric static spike ASs have the same dependence on ϵ, so we will concentrate mostly on the three-dimensional AS.

For the three-dimensional radially symmetric static spike AS, the small deviations $\delta\theta = \theta - \theta_0$ and $\delta\eta = \eta - \eta_0$ in the spherical coordinates can be taken as

$$\delta\theta = e^{\mathrm{i}\omega t} Y_{nm}(\vartheta,\varphi)\delta\theta_{n\omega}(r), \quad \delta\eta = e^{\mathrm{i}\omega t} Y_{nm}(\vartheta,\varphi)\delta\eta_{n\omega}(r), \tag{3.1}$$

where Y_{nm} are the spherical harmonics. In [30], we found that the radially symmetric static spike ASs exist in the Gray–Scott model when $A \sim \epsilon$. Using the inner solutions $\tilde\theta = \epsilon\theta_0$ and $\tilde\eta = \eta_0$ found in [30] and the variable $\tilde A = \epsilon^{-1}A$, we can write (1.8) and (1.9) linearized around θ_0 and η_0 as

$$\left[-\frac{d^2}{dr^2} - \frac{2}{r}\frac{d}{dr} + \frac{n(n+1)}{r^2} + 1 + \mathrm{i}\omega - 2\tilde A\tilde\theta\tilde\eta\right]\delta\theta_{n\omega} = \epsilon^{-1}\tilde A\tilde\theta^2\delta\eta_{n\omega}, \tag{3.2}$$

$$\left[-\frac{d^2}{dr^2} - \frac{2}{r}\frac{d}{dr} + \frac{n(n+1)}{r^2} + \epsilon^2 + \mathrm{i}\epsilon^2\alpha^{-1}\omega\right]\delta\eta_{n\omega} = -\epsilon\tilde A^{-1}\left[-\frac{d^2}{dr^2} - \frac{2}{r}\frac{d}{dr} + \frac{n(n+1)}{r^2} + 1 + \mathrm{i}\omega\right]\delta\theta_{n\omega}. \tag{3.3}$$

Equation (3.3) can be solved by means of Green's function, which, in the case of the operator in the left-hand side of (3.3) multiplied by r^2, is (a similar Green's function was used in [27, 28])

$$G_{n\omega}(r,r') = \begin{cases} \dfrac{I_{n+1/2}(\epsilon r\sqrt{1+\mathrm{i}\alpha^{-1}\omega})K_{n+1/2}(\epsilon r'\sqrt{1+\mathrm{i}\alpha^{-1}\omega})}{\sqrt{rr'}}, & r \le r', \\ \dfrac{I_{n+1/2}(\epsilon r'\sqrt{1+\mathrm{i}\alpha^{-1}\omega})K_{n+1/2}(\epsilon r\sqrt{1+\mathrm{i}\alpha^{-1}\omega})}{\sqrt{rr'}}, & r \ge r', \end{cases} \tag{3.4}$$

where $I_{n+1/2}(x)$ and $K_{n+1/2}(x)$ are the modified Bessel functions. Solving (3.3) with the use of (3.4), we obtain

$$\delta\eta_{n\omega} = -\epsilon\tilde A^{-1}\delta\theta_{n\omega} - \epsilon\tilde A^{-1}(1 - \epsilon^2 + \mathrm{i}\omega - \mathrm{i}\epsilon^2\alpha^{-1}\omega)\int_0^\infty G_{n\omega}(r,r')\delta\theta_{n\omega}(r')r'^2 dr'. \tag{3.5}$$

Substituting this expression into (3.2), we obtain the following equation:

$$\left[-\frac{d^2}{dr^2} - \frac{2}{r}\frac{d}{dr} + \frac{n(n+1)}{r^2} + 1 + \mathrm{i}\omega - 2\tilde A\tilde\theta\tilde\eta + \tilde\theta^2\right]\delta\theta_{n\omega} = -\tilde\theta^2(1 - \epsilon^2 + \mathrm{i}\omega - \mathrm{i}\epsilon^2\alpha^{-1}\omega)\int_0^\infty G_{n\omega}(r,r')\delta\theta_{n\omega}(r')r'^2 dr'. \tag{3.6}$$

This equation determines the complex frequencies of different fluctuations as the functions of the control parameters and has to be solved as an eigenvalue problem. The instability of the AS will occur when Re $\gamma < 0$, with $\gamma = -\mathrm{i}\omega$.

3.1. Case $\alpha \gg \epsilon^2$: Instability with respect to the non radially symmetric fluctuations. Let us first look at (3.6) at $\alpha \gg \epsilon^2$. In this case, the terms proportional to α^{-1} in the right-hand side of (3.6) can be neglected, so Green's function $G_{n\omega}$ can be expanded in ϵ. Then (3.6) becomes asymptotically

$$\left[-\frac{d^2}{dr^2} - \frac{2}{r}\frac{d}{dr} + \frac{n(n+1)}{r^2} + 1 - \gamma_n - 2\tilde{A}\tilde{\theta}\tilde{\eta} + \tilde{\theta}^2\right]\delta\theta_n = -\frac{\tilde{\theta}^2(r)(1-\gamma_n)}{2n+1}\int_0^\infty g_n(r,r')\delta\theta_n(r')r'dr', \tag{3.7}$$

where

$$g_n(r,r') = \begin{cases} (r/r')^n, & r \le r', \\ (r'/r)^{n+1}, & r \ge r'. \end{cases} \tag{3.8}$$

The operator in the left-hand side of (3.7) is a Schrödinger-type operator with the attractive potential $-2\tilde{A}\tilde{\theta}\tilde{\eta}$, repulsive potential $\tilde{\theta}^2$, and the centrifugal potential $n(n+1)/r^2$.

As in the case of the one-dimensional AS, the modes $\delta\theta_n$ that can lead to instabilities are localized. The numerical solution of (3.7) shows that at $\alpha \gg \epsilon^2$ the AS is stable in a certain range $\tilde{A}_b < \tilde{A} < \tilde{A}_{c2}$. The value of $\tilde{A}_b \simeq 5.8$ coincides with the boundary of existence of the AS [30] and corresponds to the fluctuation with $n = 0$. This fluctuation leads to the AS collapse [29, 32]. At $\tilde{A} = \tilde{A}_{c2} \simeq 8.4$, there is an instability with respect to the mode with $n = 2$.

The presence of the localized solution $\delta\theta_n$ of (3.7) with $\gamma_n = 0$ for $n > 0$ signifies an instability of the radially symmetric static AS with respect to the non radially symmetric fluctuations resulting in the distortions of the spike and leading to its splitting [29, 32]. It is clear that this instability will occur more easily at smaller values of n. (Note that the case $n = 1$ corresponds to the translation of the AS as a whole and therefore does not lead to any distortions.) The numerical solution of (3.7) shows that the AS first becomes unstable with respect to the fluctuation with $n = 2$. All other modes go unstable at higher values of $\tilde{A}$.

It is not difficult to show that for $\tilde{A} \gg 1$ the AS will be unstable with respect to the fluctuations with $n \neq 0$. Indeed, according to the results of [30], for these values of $\tilde{A}$, the AS has the form of an annulus of large radius $R \sim \tilde{A}^2$. Using the analytical expressions for $\tilde{\theta}$ and $\tilde{\eta}$ obtained in [30] in this case, one can see that the leading contribution to the potential in the left-hand side of (3.7) is $V(r) \cong -3\cosh^{-2}\left(\frac{r-R}{2}\right)$. For $R \gg 1$ and $1 \ll n \ll R$, all of the other terms can be considered as a perturbation to the Schrödinger operator with this potential, and so to the leading order of the perturbation theory for the lowest eigenvalue of the Schrödinger operator we have $\delta\theta = \delta\theta_0(r-R)$, where $\delta\theta_0(x)$ is given by (A.2), and we moved the boundary condition at $r = 0$ to minus infinity. In the first order of the perturbation theory, we obtain

$$\gamma_n \simeq \left(-\frac{5}{4} + \frac{n^2}{R^2} + \frac{225\pi^2}{2048n}\right)\left(1 + \frac{225\pi^2}{2048n}\right)^{-1}. \tag{3.9}$$

This equation shows that for $R \gg 1$ there is a range of values of n for which $\gamma_n < 0$. The fact that the annulus must be unstable with respect to the shape deformations is

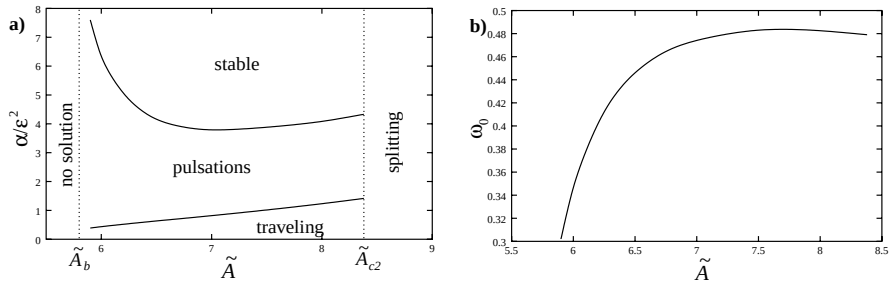

FIG. 3.1. (a) *The stability diagram for the three-dimensional radially symmetric AS.* (b) *The frequency ω_0 at the threshold of the pulsation instability. Results of the numerical solution of* (3.6). *In* (a), *the upper solid line shows the values of α_ω/ϵ^2 corresponding to the onset of the pulsation instability ($n = 0$), and the lower solid curve shows the values of α_T/ϵ^2 corresponding to the instability leading to the onset of traveling motion ($n = 1$). The dotted lines correspond to the instabilities of the static AS at $\tilde{A} = \tilde{A}_b$ and $\tilde{A} = \tilde{A}_{c2}$.*

an obvious consequence of its quasi-one-dimensional character (see section 2.3). It is interesting to note that (3.9) with $n = 2$, together with the expression for $R(\tilde{A})$ from [30], gives the correct value of $\tilde{A}_{c2}$ with accuracy better than 5%.

Dynamically, when the value of A is increased beyond the value corresponding to $\tilde{A}_{c2}$, the buildup of the instability with $n = 2$ will result in splitting of the AS [32, 38]. After such a splitting event, the two newborn ASs will go apart until they are separated by a sufficiently large distance and then will split again. Thus the considered instability will result in self-replication of ASs [29, 32, 38]. We would like to emphasize that the character of the instability that leads to self-replication in three-dimensional (and two-dimensional) systems is significantly different from that in one dimension. In the former, the instability results in the buildup of the *shape* distortion that eventually leads to splitting, while, in the latter, the instability leads to the widening of the activator distribution profile and *local breakdown* in the AS center (see section 2.1). Thus self-replication of the AS in one dimension is qualitatively different from that in higher dimensions. Similar conclusions were made in a wide class of reaction-diffusion models [26, 27, 28].

3.2. Case $\alpha \lesssim \epsilon^2$: Instability with respect to pulsations and the onset of traveling motion. According to the general qualitative theory of ASs, when α becomes small, the AS may become unstable with respect to pulsations with $\mathrm{Re}\,\omega \neq 0$. The analysis of (3.6) with $n = 0$ shows that this instability may be realized only when $\alpha \sim \epsilon^2$ and $\mathrm{Re}\,\omega = \omega_0 \sim 1$. In view of this fact, we can drop 1 in the square roots in (3.4). Equation (3.6) can then be solved numerically. The results of this numerical solution are presented in Figure 3.1. The upper curve in Figure 3.1(a) shows the critical values of α_ω for the onset of this instability for those values of $\tilde{A}$ at which the AS is stable at $\alpha \gg \epsilon^2$. Figure 3.1(b) shows the frequency ω_0 of the fluctuations at the threshold of the instability. From Figure 3.1(a), one can see that the static three-dimensional AS is unstable for all values of $\tilde{A}$ if $\alpha < \alpha_c \simeq 3.7\epsilon^2$.

In addition to the modes studied above, we always have a dangerous mode $\delta\theta = d\tilde{\theta}/dr$ with $n = 1$ corresponding to translations. The analysis of (3.6) shows that, in addition to the trivial solution, at some $\alpha = \alpha_T \sim \epsilon^2$, this equation can have another solution with $\gamma = 0$. As in the case of the one-dimensional AS, this solution will

signify the instability which results in the AS starting to move as a whole. To find this instability point, we need to know the behavior of Green's function $G_{1\omega}(r, r')$ at small values of $\mathrm{i}\omega$. Expanding the Bessel functions in (3.4) and finding the adjoint function $\delta\theta_1^*$ numerically, we calculate the coefficient in front of $\mathrm{i}\omega$ in the first order of the perturbation theory, keeping only the leading terms in ϵ. The above-mentioned instability will be realized when this coefficient vanishes. The lower solid line in Figure 3.1(a) shows the values of α_T/ϵ^2 at which this happens. One can see that this instability occurs when the AS is already unstable with respect to pulsations. Note that the numerical solution of (3.6) shows that the instabilities with respect to the fluctuations with $n \geq 2$ always happen for significantly lower values of α.

4. Stability of the two-dimensional radially symmetric static spike AS. Finally, we will briefly discuss the stability of the two-dimensional static spike AS for $\epsilon \ll 1$. In the cylindrical coordinates r, φ, the small deviations $\delta\theta = \theta - \theta_0$ and $\delta\eta = \eta - \eta_0$ can be taken as

$$\delta\theta = \delta\theta_{n\omega}(r)e^{\mathrm{i}\omega t - \mathrm{i}n\varphi}, \quad \delta\eta = \delta\eta_{n\omega}(r)e^{\mathrm{i}\omega t - \mathrm{i}n\varphi}, \tag{4.1}$$

where n is an integer.

The equation for $\delta\theta_{n\omega}$ is obtained by linearizing (1.8) and (1.9) around θ_0 and η_0 and eliminating $\delta\eta_{n\omega}$ by inverting the equation for $\delta\eta_{n\omega}$. As a result, using the inner solutions $\tilde{\theta} = \epsilon\theta_0$ and $\tilde{\eta} = \eta_0 \ln \epsilon^{-1}$ and the variable $\tilde{A} = A/(\epsilon \ln \epsilon^{-1})$ obtained in [30], we arrive at the following equation for $\delta\theta_{n\omega}$:

$$\begin{aligned} &\left[-\frac{d^2}{dr^2} - \frac{1}{r}\frac{d}{dr} + \frac{n^2}{r^2} + 1 + \mathrm{i}\omega - 2\tilde{A}\tilde{\theta}\tilde{\eta} + \tilde{\theta}^2\right]\delta\theta_{n\omega} \\ &\qquad = -\tilde{\theta}^2(1 - \epsilon^2 + \mathrm{i}\omega - \mathrm{i}\epsilon^2\alpha^{-1}\omega)\int_0^\infty G_{n\omega}(r, r')\delta\theta_{n\omega}(r')r'dr', \end{aligned} \tag{4.2}$$

where $G_n(r, r')$ is given by

$$G_n(r, r') = \begin{cases} I_n(\epsilon r\sqrt{1 + \mathrm{i}\alpha^{-1}\omega})K_n(\epsilon r'\sqrt{1 + i\alpha^{-1}\omega}), & r < r', \\ I_n(\epsilon r'\sqrt{1 + \mathrm{i}\alpha^{-1}\omega})K_n(\epsilon r\sqrt{1 + \mathrm{i}\alpha^{-1}\omega}), & r > r', \end{cases} \tag{4.3}$$

where I_n and K_n are the modified Bessel functions. The analysis of this equation can be performed in the way completely analogous to that of (3.6). It is clear that the instabilities of the two-dimensional static spike AS will be qualitatively the same as those of the three-dimensional AS. We would like to emphasize that, as in the case of the three-dimensional AS, splitting and self-replication of the static spike AS in the two-dimensional system is related to the buildup of the fluctuation with $n = 2$ describing a nonsymmetric distortion of the AS. Because of the very slow convergence of the asymptotic theory in two dimensions (recall that the small parameter here is $1/\ln \epsilon^{-1}$), we will not present a detailed study of (4.2).

Note that Wei studied existence and stability of the two-dimensional radially symmetric static spike ASs in the Gray–Scott model with $A \sim \epsilon \ln^{1/2} \epsilon^{-1}$ [41]. This regime differs from the one studied by us only by logarithmic factors. The stability results of Wei agree with ours up to the logarithmic terms.

5. Conclusion. In conclusion, we performed a comprehensive linear stability analysis of the static spike ASs in the Gray–Scott model for $\epsilon \ll 1$.

We found that the one-dimensional static spike ASs are stable in one dimension for $\alpha > 0.33$ in the entire region of their existence $3.46\epsilon^{1/2} \leq A \leq 1.35$. At $A = 3.46\epsilon^{1/2}$,

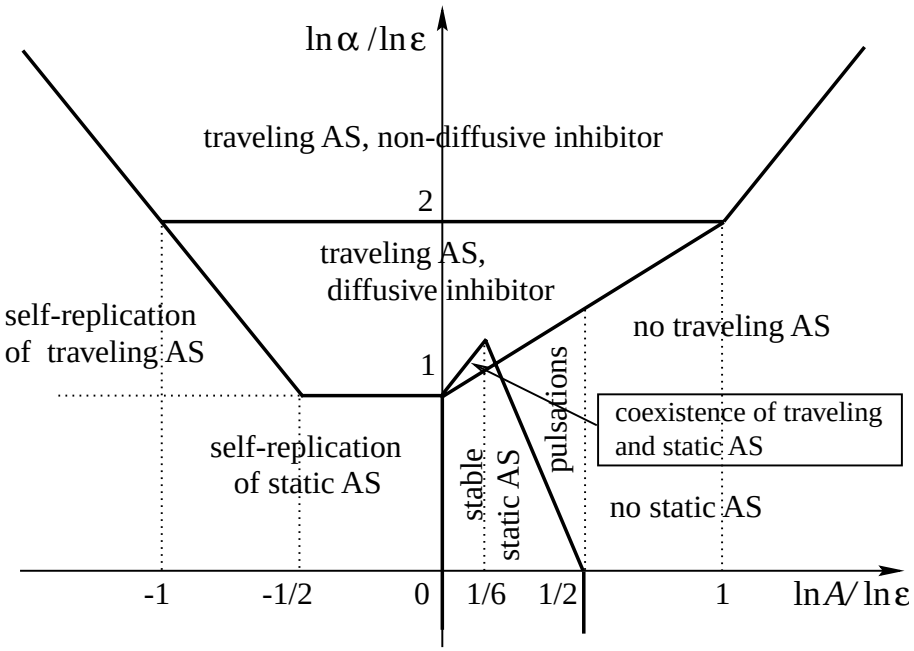

FIG. 5.1. *The diagram of existence and stability of different ASs in one dimension in the limit* $\epsilon \to 0$.

the AS collapses into the homogeneous state, while, at $A = 1.35$, a local breakdown in the center of the AS occurs, leading to its splitting [29, 30, 39, 40].

When the value of α is decreased, the AS can undergo two types of instabilities in one dimension. If $A < 1.58\epsilon^{1/6}$, the AS destabilizes with respect to pulsations and, after a few periods, collapses to the homogeneous state [29]. If, on the other hand, $A > 1.58\epsilon^{1/6}$, the AS will destabilize with respect to the onset of traveling motion and transform to a traveling AS [29]. At $\alpha < 0.83\epsilon^{4/3}$, the static one-dimensional spike AS is unstable for all values of the parameters.

The results on the existence of the static spike ASs and their stability in one dimension obtained in the previous sections, together with the results of [31] on the existence of the traveling spike ASs, are summarized in Figure 5.1. This figure shows the domains of existence and the instability lines for the ASs in the $\ln \alpha - \ln A$ plane in the limit $\epsilon \to 0$.

The analysis of stability of the one-dimensional static spike ASs (stripes) in higher dimensions shows that these ASs are always unstable with respect to both the corrugation and wriggling instabilities, which results in the granulation of the stripes [29, 32].

The three-dimensional radially symmetric static spike ASs are stable in a narrow range $5.8\epsilon < A < 8.4\epsilon$ when $\alpha \gg \epsilon^2$. At $A = 5.8\epsilon$, the AS collapses into the homogeneous state, while, at $A = 8.4\epsilon$, it destabilizes with respect to the deformation, which leads to its splitting [29, 32]. When the value of α is decreased, at some $\alpha_\omega \sim \epsilon^2$, the AS undergoes a pulsation instability. For $\alpha < 3.7\epsilon^2$, the three-dimensional radially symmetric spike ASs are unstable for all values of the parameters. Similar conclusions can be made about the two-dimensional radially symmetric ASs.

Appendix A. Analysis of (2.8). Equation (2.8) is of the kind studied by Kerner and Osipov in the case of the ASs in systems of small size [6, 11, 15, 18, 21, 22, 23]. Here we perform a rigorous analysis of (2.8) using their method.

Let us introduce the orthonormal basis set $\delta\theta_n$ of the eigenfunctions of the Schrödinger operator in the left-hand side of (2.8)

$$\left[-\frac{d^2}{dx^2}+1-3\cosh^{-2}\left(\frac{x}{2}\right)\right]\delta\theta_n=\lambda_n\delta\theta_n. \tag{A.1}$$

This operator has three discrete eigenvalues

$$\begin{aligned}
&\lambda_0=-\frac{5}{4}, \quad \delta\theta_0=\sqrt{\frac{15}{32}}\cosh^{-3}\left(\frac{x}{2}\right),\\
&\lambda_1=\ 0, \qquad \delta\theta_1=\sqrt{\frac{15}{8}}\tanh\left(\frac{x}{2}\right)\cosh^{-2}\left(\frac{x}{2}\right),\\
&\lambda_2=\ \frac{3}{4}, \qquad \delta\theta_2=\sqrt{\frac{3}{32}}\left(5\tanh^2\left(\frac{x}{2}\right)-1\right)\cosh^{-1}\left(\frac{x}{2}\right),
\end{aligned} \tag{A.2}$$

and a continuous spectrum for $\lambda_n>1$ [24].

Assuming for a moment that the problem is considered on a large but finite domain, we can write the operators of (2.8) in this basis as

$$B_{mn}=(\lambda_n-\gamma)\delta_{mn}+C(1-\gamma)b_m^l b_n^r, \tag{A.3}$$

where δ_{mn} is the Kronecker delta,

$$b_n^l=\int_{-\infty}^{+\infty}\cosh^{-4}\left(\frac{x}{2}\right)\delta\theta_n(x)dx, \quad b_n^r=\int_{-\infty}^{+\infty}\delta\theta_n(x)dx, \tag{A.4}$$

and

$$C=\frac{3A^2}{8A_b^2}\left(1+\sqrt{1-\frac{A_b^2}{A^2}}\right)^2. \tag{A.5}$$

Observe that C is a monotonically increasing function of $A\geq A_b$.

In terms of B_{mn}, (2.8) becomes

$$\det B_{mn}=0. \tag{A.6}$$

Note that, since by symmetry b_n^l and b_n^r are identically zero for odd functions $\delta\theta_n$, we immediately conclude that these functions are the solutions of (2.8) with $\gamma_n=\lambda_n$ corresponding to these functions.

It is not difficult to show that because of the special form of the second matrix in (A.3) we have [6, 11, 15, 18, 21, 22, 23] (see also [1])

$$\det B_{mn}=\left[1+C(1-\gamma)\sum_n\frac{a_n}{\lambda_n-\gamma}\right]\prod_n(\lambda_n-\gamma), \tag{A.7}$$

where $a_n=b_n^l b_n^r$ and the summation is over the even states only. Using (A.1), one can bring the expression for a_n to a symmetric form which is convenient for further calculations:

$$a_n=\frac{2\lambda_n}{\lambda_n-1}\left[\int_{-\infty}^{+\infty}\cosh^{-2}\left(\frac{x}{2}\right)\delta\theta_n(x)dx\right]^2. \tag{A.8}$$

The values of a_0 and a_2 can be calculated explicitly with the use of (A.2):

$$a_0 = \frac{75\pi^2}{256}, \quad a_2 = -\frac{9\pi^2}{256}. \tag{A.9}$$

The calculation of a_k corresponding to the functions $\delta\theta_k$ of the continuous spectrum (with the wave vector k and $\lambda_k = 1 + k^2$) is rather involved. The functions $\delta\theta_k$ can be written as linear combinations of the real and the imaginary parts of

$$u(y) = (1 - y^2)^{\mathrm{i}k} F\left(2\mathrm{i}k - 3, 2\mathrm{i}k + 4, 2\mathrm{i}k + 1, \frac{1 - y}{2}\right), \tag{A.10}$$

where $y = \tanh(x/2)$ and $F(\alpha, \beta, \gamma, x)$ is the hypergeometric function [24], to obtain the even functions $\delta\theta_k$. The functions $\delta\theta_k$ should be normalized in such a way that $\delta\theta_k(x) \to \cos(kx \pm \delta)$ as $x \to \pm\infty$. Then, after calculating the respective integrals, we arrive at

$$a_k = \frac{8\pi^2 k^2 (k^2 + 1)}{(16k^4 + 40k^2 + 9)\sinh^2(\pi k)} > 0. \tag{A.11}$$

Naturally, in the infinite domain, one should replace the summation over the continuous spectrum in (A.7) by integration: $\sum_n \to \int_0^\infty \frac{dk}{\pi}$.

To study the unstable solutions of (A.6), we need to analyze zeros of the function

$$D(\omega) = 1 + C(1 + \mathrm{i}\omega)\left(\frac{a_0}{\lambda_0 + \mathrm{i}\omega} + \frac{a_2}{\lambda_2 + \mathrm{i}\omega} + \int_0^\infty \frac{a_k dk}{\pi(1 + k^2 + \mathrm{i}\omega)}\right) \tag{A.12}$$

in the lower half-plane of the complex frequency $\omega = \mathrm{i}\gamma$. This can be done with the aid of the argument principle [6, 11, 15, 18, 21, 22, 23] which states that the number of zeros N of the complex function $D(\omega)$ in this region of the complex frequency ω is equal to

$$N = P + \frac{1}{2\pi}\Delta \arg D(\omega), \tag{A.13}$$

where P is the number of poles there and $\Delta \arg D(\omega)$ is the change of the argument of the function $D(\omega)$ as ω winds around this region of the complex frequency counterclockwise.

From the spectrum of the operator in (A.1), one can see that only the pole at $\omega = \mathrm{i}\lambda_0$ lies in the lower half-plane of the complex frequency, so we have $P = 1$ [6, 11, 15, 18, 21, 22, 23]. Let us see how the function $D(\omega)$ with ω real varies as ω goes from $+\infty$ to $-\infty$. Since $D(\omega)$ is symmetric with respect to the real axis, one needs only to analyze the case of positive ω. At $\omega = \infty$, we have

$$D(\infty) = 1 + C\left(a_0 + a_2 + \int_0^\infty \frac{a_k dk}{\pi}\right) > 0, \tag{A.14}$$

where we used the explicit expressions for $a_{0,2,k}$ and $\lambda_{0,2}$ to calculate the sign of $D(\infty)$ and evaluated the integral in this equation to be $\int_0^\infty \pi^{-1} a_k dk \simeq 0.12$. On the other hand, at $\omega = 0$, we have

$$D(0) = 1 + C\left(\frac{a_0}{\lambda_0} + \frac{a_2}{\lambda_2} + \int_0^\infty \frac{a_k dk}{\pi(1 + k^2)}\right) = 1 - \frac{8}{3}C < 0 \tag{A.15}$$

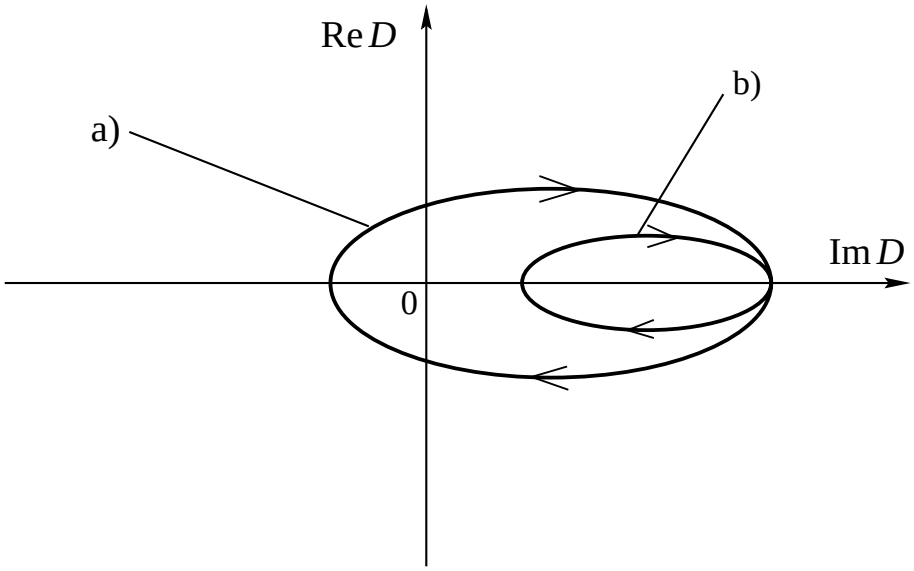

FIG. A.1. *The behavior of the function $D(\omega)$ for the static AS* (a) *and for the small amplitude solution from* [30] (b).

for $A > A_b$. The latter expression can be obtained by recalling that at $A = A_b$, for which $C = 3/8$, we have $D(0) = 0$ (see section 2), and C monotonically increases with A.

It is not difficult to show that the imaginary part of $D(\omega)$ is negative for all $\omega > 0$:

$$\begin{aligned}\frac{\text{Im } D(\omega)}{C\omega} &= \frac{a_0(\lambda_0 - 1)}{\lambda_0^2 + \omega^2} + \frac{a_2(\lambda_2 - 1)}{\lambda_2^2 + \omega^2} + \int_0^\infty \frac{k^2 a_k dk}{\pi[(1+k^2)^2 + \omega^2]} \\ &< \frac{a_0(\lambda_0 - 1)}{\lambda_0^2 + \omega^2} + \frac{1}{\lambda_2^2 + \omega^2}\left(a_2(\lambda_2 - 1) + \int_0^\infty \frac{k^2 a_k dk}{\pi}\right) < 0. \end{aligned} \tag{A.16}$$

The last inequality is obtained by using the explicit expressions for $a_{0,2,k}$, $\lambda_{0,2}$ and the evaluation of the last integral $\int_0^\infty \pi^{-1} k^2 a_k dk \simeq 0.02$. Note that, because of the smallness of the contributions from the continuous spectrum, one can get very good approximations for the solutions of (2.8) by restricting $\delta\theta_n$ to the discrete spectrum only (see also [36, 37]).

From all this, we conclude that the function $D(\omega)$ has the form shown in Figure A.1(a), so we have $\Delta \arg D(\omega) = -2\pi$ for the static spike AS. This means that $N = 0$, and (2.8) does not have solutions with Re $\gamma < 0$. Note that the same line of arguments shows that the asymptotic stability problem for the stationary solution with the smaller amplitude for $A \sim A_b$ found in [30] always has a solution with Re $\gamma < 0$ since in that case $\Delta \arg D(\omega) = 0$ (see Figure A.1(b)). So this small-amplitude solution is always unstable. These conclusions are in agreement with the general qualitative theory of the ASs [21, 22, 23].

Appendix B. Analysis of (2.10). In this section, we use the method of the previous section to analyze the solutions of (2.10). This method was used by Kerner and Osipov for studying the instabilities of the static ASs for small values of α in systems of small size [16, 19, 20, 21, 22, 23].

After introducing the orthonormal basis set of the eigenfunctions of (A.1), we get the following expression for B_{mn} from (2.10):

$$B_{mn} = (\lambda_n + \mathrm{i}\omega)\delta_{mn} + C\frac{1+\mathrm{i}\omega}{\sqrt{\mathrm{i}\omega+\alpha}} b_m^l b_n^r, \tag{B.1}$$

where now

$$C = \frac{A^2\alpha^{1/2}}{8\epsilon}; \tag{B.2}$$

the rest is the same as in (A.3), and $\alpha \to +0$ (cf. (2.6); α will determine the proper winding direction; see below). As in the previous section, we may write

$$\det B_{mn} = \left[1 + C\frac{1+\mathrm{i}\omega}{\sqrt{\mathrm{i}\omega+\alpha}} \sum_n \frac{a_n}{\lambda_n + \mathrm{i}\omega}\right] \prod_n (\lambda_n - \gamma), \tag{B.3}$$

where a_n are given by (A.8). To analyze the solutions of (A.6) with these B_{mn}, we will study zeros of the function

$$D(\omega) = 1 + C\frac{1+\mathrm{i}\omega}{\sqrt{\mathrm{i}\omega+\alpha}} \left(\frac{a_0}{\lambda_0+\mathrm{i}\omega} + \frac{a_2}{\lambda_2+\mathrm{i}\omega} + \int_0^\infty \frac{a_k dk}{\pi(1+k^2+\mathrm{i}\omega)}\right), \tag{B.4}$$

where a_k are given by (A.11), in the lower half-plane of the complex frequency ω by using the argument principle ((A.13), in which, as before, $P = 1$). Of course, as in the previous section, $D(\omega)$ should be symmetric with respect to the real axis.

For $\omega > 0$, the real and the imaginary parts of $D(\omega)$ can be written as

$$\begin{aligned}\mathrm{Re}\ \frac{\sqrt{2\omega}}{C} D(\omega) = {} & \frac{\sqrt{2\omega}}{C} + (1+\omega)\left(\frac{a_0\lambda_0}{\lambda_0^2+\omega^2} + \frac{a_2\lambda_2}{\lambda_2^2+\omega^2} + \int_0^\infty \frac{(1+k^2)a_k dk}{\pi[(1+k^2)^2+\omega^2]}\right) \\ & + \omega(1-\omega)\left(-\frac{a_0}{\lambda_0^2+\omega^2} - \frac{a_2}{\lambda_2^2+\omega^2} - \int_0^\infty \frac{a_k dk}{\pi[(1+k^2)^2+\omega^2]}\right)\end{aligned} \tag{B.5}$$

and

$$\begin{aligned}\mathrm{Im}\ \frac{\sqrt{2\omega}}{C} D(\omega) = {} & \omega(1+\omega)\left(-\frac{a_0}{\lambda_0^2+\omega^2} - \frac{a_2}{\lambda_2^2+\omega^2} - \int_0^\infty \frac{a_k dk}{\pi[(1+k^2)^2+\omega^2]}\right) \\ & + (\omega-1)\left(\frac{a_0\lambda_0}{\lambda_0^2+\omega^2} + \frac{a_2\lambda_2}{\lambda_2^2+\omega^2} + \int_0^\infty \frac{(1+k^2)a_k dk}{\pi[(1+k^2)^2+\omega^2]}\right).\end{aligned} \tag{B.6}$$

Using the explicit expressions for $a_{0,2,k}$ and $\lambda_{0,2}$ from the previous section, it is not difficult to show that the expressions in the brackets in (B.6) are negative for all values of ω. The analysis of (B.6) then shows that Im $D(\omega)$ should change sign only once when $0 < \omega < \infty$. Let us denote the value of ω at which this happens as ω_0. Note that, according to (B.6), we must have $\omega_0 < 1$.

From the definition of $D(\omega)$, one can see that

$$D(\omega) \to 1 + C\frac{1 \mp \mathrm{i}}{\sqrt{2|\omega|}} \left(a_0 + a_2 + \int_0^\infty \frac{a_k dk}{\pi}\right), \quad \omega \to \pm\infty. \tag{B.7}$$

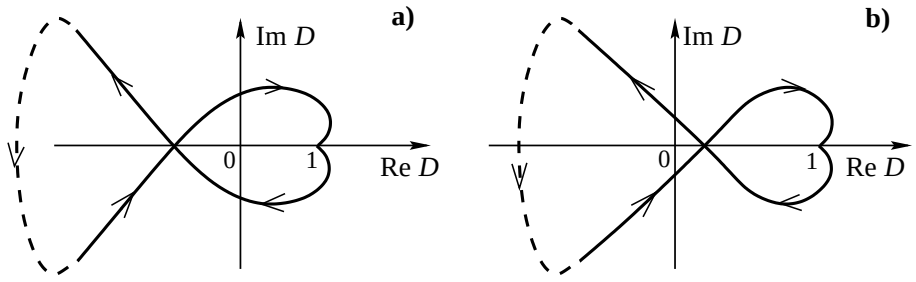

FIG. B.1. *A qualitative form of the function $D(\omega)$ for large values of C* (a) *and for small values of C* (b).

Since the expression in the brackets in this equation is positive, we will have Im $D(\omega) < 0$ for sufficiently large $\omega > 0$. On the other hand,

$$D(\omega) \to \frac{8C(-1 \pm \mathrm{i})}{3\sqrt{2|\omega|}}, \quad \omega \to \pm 0. \tag{B.8}$$

Therefore, for sufficiently small $\omega > 0$, we must have Im $D(\omega) > 0$. Observe that (B.8) was obtained for $\alpha = 0$. When α is small but finite, the two branches in (B.8) will actually get connected at Re $D(\omega) \sim -\alpha^{-1/2}$. Thus the qualitative behavior of $D(\omega)$ should be the one shown in Figure B.1. Note that the function $D(\omega)$ can be calculated numerically from (B.4) for any value of C and has indeed the form shown in Figure (B.1).

The number of zeros of $D(\omega)$ in the lower half-plane of the complex frequency is determined by Re $D(\omega_0)$. According to (B.4), if C is sufficiently small, the first term in (B.5) will dominate for $\omega = \omega_0$, and so we will have Re $D(\omega_0) > 0$. In this case, the change of the argument of $D(\omega)$ will be $\Delta \arg D(\omega) = 2\pi$ (Figure B.1(a)), so we will have $N = 2$ and therefore an instability. On the other hand, if C is large, we can neglect $\sqrt{2\omega}/C$ at $\omega = \omega_0$ in (B.5). From (B.5) and the fact that $\omega_0 < 1$, one can then see that Re $D(\omega_0) < 0$. In this case, the change of the argument will be $\Delta \arg D(\omega) = -2\pi$ (Figure B.1(b)), so the number of zeros in the lower half-plane is $N = 0$, implying stability. From all of this, we see that as the value of C is decreased, at some $C = C_0$, a complex-conjugate pair of unstable solutions of (2.10) appears, signifying a Hopf bifurcation. The numerical analysis of (B.4) shows that $C_0 \simeq 0.2837$, which corresponds to $\alpha_\omega \simeq 5.15\epsilon^2 A^{-4}$ and $\omega_0 \simeq 0.534$, in excellent agreement with the results of section 2.2.

REFERENCES

[1] A. BOSE AND G. A. KRIEGSMANN, *Stability of localized structures in non-local reaction-diffusion equations*, Methods Appl. Anal., 5 (1998), pp. 351–366.

[2] M. C. CROSS AND P. S. HOHENBERG, *Pattern formation outside of equilibrium*, Rev. Modern Phys., 65 (1993), pp. 851–1112.

[3] J. D. DOCKERY AND J. P. KEENER, *Diffusive effects on dispersion in excitable media*, SIAM J. Appl. Math., 49 (1989), pp. 539–566.

[4] A. DOELMAN, R. A. GARDNER, AND T. J. KAPER, *Stability analysis of singular patterns in the 1D Gray-Scott model: A matched asymptotics approach*, Phys. D, 122 (1998), pp. 1–36.

[5] A. DOELMAN, T. J. KAPER, AND P. ZEGELING, *Pattern formation in the one-dimensional Gray-Scott model*, Nonlinearity, 10 (1997), pp. 523–563.

[6] A. L. Dubitskii, B. S. Kerner, and V. V. Osipov, *Two types of spike autosolitons*, Soviet Phys. Dokl., 34 (1989), pp. 906–908.
[7] R. J. Field and M. Burger, eds., *Oscillations and Traveling Waves in Chemical Systems*, Wiley, New York, 1985.
[8] P. Gray and S. Scott, *Autocatalytic reactions in the isothermal continuous stirred tank reactor*, Chem. Engrg. Sci., 38 (1983), pp. 29–43.
[9] J. K. Hale, L. A. Peletier, and W. C. Troy, *Exact homoclinic and heteroclinic solutions of the Gray–Scott model for autocatalysis*, SIAM J. Appl. Math., 61 (2000), pp. 102–130.
[10] R. Kapral and K. Showalter, *Chemical Waves and Patterns*, Kluwer, Dordrecht, 1995.
[11] B. S. Kerner and V. V. Osipov, *Nonlinear theory of stationary strata in dissipative systems*, Sov. Phys. – JETP, 47 (1978), pp. 874–885.
[12] B. S. Kerner and V. V. Osipov, *Striations in a heated electron-hole plasma*, Sov. Phys. – Semicond., 13 (1979), pp. 424–431.
[13] B. S. Kerner and V. V. Osipov, *Stochastically inhomogeneous structures in nonequilibrium systems*, Sov. Phys. – JETP, 52 (1980), pp. 1122–1132.
[14] B. S. Kerner and V. V. Osipov, *Stationary and traveling dissipative structures in active kinetic media*, Mikroelektronika, 10 (1981), pp. 407–432 (in Russian).
[15] B. S. Kerner and V. V. Osipov, *Properties of stationary dissipative structures in mathematical models of morphogenesis*, Biophysics (USSR), 27 (1982), pp. 138–143.
[16] B. S. Kerner and V. V. Osipov, *Pulsating heterophase regions in nonequilibrium systems*, Sov. Phys. – JETP, 56 (1982), pp. 1275–1282.
[17] B. S. Kerner and V. V. Osipov, *Traveling heterophase regions in nonequilibrium systems*, Mikroelektronika, 12 (1983), pp. 512–529 (in Russian).
[18] B. S. Kerner and V. V. Osipov, *Highly nonequilibrium localized states in systems slightly away from thermodynamic equilibrium*, Sov. Phys. – JETP Lett., 41 (1985), pp. 473–475.
[19] B. S. Kerner and V. V. Osipov, *Autosolitons in a hot semiconductor plasma*, Sov. Phys. – JETP, 62 (1985), pp. 337–348.
[20] B. S. Kerner and V. V. Osipov, *Autosolitons in active systems with diffusion*, in Nonlinear Irreversible Processes, W. Ebeling and H. Ulbricht, eds., Springer-Verlag, Berlin, 1986.
[21] B. S. Kerner and V. V. Osipov, *Autosolitons*, Sov. Phys. – Usp., 32 (1989), pp. 101–138.
[22] B. S. Kerner and V. V. Osipov, *Self-organization in active distributed media*, Sov. Phys. – Usp., 33 (1990), pp. 679–719.
[23] B. S. Kerner and V. V. Osipov, *Autosolitons: A New Approach to Problem of Self-Organization and Turbulence*, Kluwer, Dordrecht, 1994.
[24] L. D. Landau and E. M. Lifshitz, *Course of Theoretical Physics*, Vol. 3, Pergamon Press, Oxford, UK, 1965.
[25] A. S. Mikhailov, *Foundations of Synergetics*, Springer-Verlag, Berlin, 1990.
[26] C. B. Muratov, *Self-replication and splitting of domain patterns in reaction-diffusion systems with the fast inhibitor*, Phys. Rev. E, 54 (1996), pp. 3369–3376.
[27] C. B. Muratov and V. V. Osipov, *General theory of instabilities for patterns with sharp interfaces in reaction-diffusion systems*, Phys. Rev. E, 53 (1996), pp. 3101–3116.
[28] C. B. Muratov and V. V. Osipov, *Scenarios of domain pattern formation in a reaction-diffusion system*, Phys. Rev. E, 54 (1996), pp. 4860–4879.
[29] C. B. Muratov and V. V. Osipov, *Spike Autosolitons in the Gray-Scott Model*, CAMS Rep. 9900-10, NJIT, Newark, NJ (available at LANL archive: patt-sol/9804001).
[30] C. B. Muratov and V. V. Osipov, *Static spike autosolitons in the Gray-Scott model*, J. Phys. A, 33 (2000), pp. 8893–8916.
[31] C. B. Muratov and V. V. Osipov, *Traveling spike autosolitons in the Gray-Scott model*, Phys. D, 155 (2001), pp. 112–131.
[32] C. B. Muratov and V. V. Osipov, *Spike autosolitons and pattern formation scenarios in the two-dimensional Gray-Scott model*, European Phys. J. B, (2001), pp. 213–221.
[33] J. D. Murray, *Mathematical Biology*, Springer-Verlag, Berlin, 1989.
[34] F. J. Niedernostheide, ed., *Nonlinear Dynamics and Pattern Formation in Semiconductors and Devices*, Springer-Verlag, Berlin, 1994.
[35] V. V. Osipov, *Criteria of spontaneous interconversions of traveling and static arbitrary-dimensional dissipative structures*, Phys. D, 93 (1996), pp. 143–156.
[36] V. V. Osipov and A. V. Severtsev, *Theory of self-replication and granulation of spike autosolitons*, Phys. Lett. A, 222 (1996), pp. 400–404.
[37] V. V. Osipov and A. V. Severtsev, *Transverse instability of spike autosolitons*, Phys. Lett. A, 227 (1997), pp. 61–66.
[38] J. E. Pearson, *Complex patterns in a simple system*, Science, 261 (1993), pp. 189–192.

[39] W. N. Reynolds, J. E. Pearson, and S. Ponce-Dawson, *Dynamics of self-replicating patterns in reaction-diffusion systems*, Phys. Rev. Lett., 72 (1994), pp. 2797–2800.
[40] W. N. Reynolds, J. E. Pearson, and S. Ponce-Dawson, *Self-replicating spots in reaction-diffusion systems*, Phys. Rev. E, 56 (1997), pp. 185–198.
[41] J. C. Wei, *Pattern formation in two-dimensional Gray-Scott model: Existence of single-spot solutions and their stability*, Phys. D, 148 (2001), pp. 20–48.